BBA - Biomembranes 1862 (2020) 183103

Contents lists available at ScienceDirect

BBA - Biomembranes

journal homepage: www.elsevier.com/locate/bbamem

Imidazolium-based ionic liquids cause mammalian cell death due to modulated structures and dynamics of cellular membrane

Karishma Bakshi[a], Saheli Mitra[b], Veerendra Kumar Sharma[c], Magani Sri Krishna Jayadev[a], Victoria Garcia Sakai[d], Ramaprasad Mukhopadhyay[c,e], Ashish Gupta[a], Sajal Kumar Ghosh[b,*]

[a] Department of Life Sciences, School of Natural Sciences, Shiv Nadar University, NH-91, Tehsil Dadri, G. B. Nagar, Uttar Pradesh 201314, India
[b] Department of Physics, School of Natural Sciences, Shiv Nadar University, NH-91, Tehsil Dadri, G. B. Nagar, Uttar Pradesh 201314, India
[c] Solid State Physics Division, Bhabha Atomic Research Centre, Mumbai 400085, India
[d] ISIS Pulsed Neutron and Muon Facility, Science and Technology Facilities Council, Rutherford Appleton Laboratory, Didcot OX11 0QX, UK
[e] Homi Bhabha National Institute, Anushaktinagar, Mumbai 400094, India

ARTICLE INFO

Keywords:
Imidazolium-based ionic liquids toxicity
Perturbed morphology of cancer liver cell
Altered membrane elasticity
Faster in-plane diffusion of lipids
Molecular mechanism of toxicity of ionic liquids

ABSTRACT

Here, we report the toxic effects of various imidazolium-based ionic liquids (ILs) with varying hydrocarbon chain lengths, on different human cell lines. Multiple biological assays have shown that the ILs with long hydrocarbon chains have stronger adverse effect especially on human liver cancer cells (Huh-7.5 cells). Further, our study has confirmed that the ILs induce necrosis dependent cell death and that it is related to cell membrane damage. To understand the molecular mechanism of such an effect, the cellular membranes were mimicked as lipid monolayers formed at the air-water interface and then as lipid bilayer vesicles. The pressure area-isotherms measured from the monolayer have shown that the interaction of ILs with the lipid layer is energetically favourable. The addition of these ILs reduces the in-plane elasticity of the self-assembled molecular layer. Quasielastic neutron scattering data clearly indicate that ILs in liver lipid vesicles significantly affects the dynamics of the lipid, in particular, the lateral motion of the lipids. It has been concluded that the mammalian cell death induced by these ILs is due to the modulated structure and altered physical properties of the cellular membrane.

1. Introduction

Room temperature ionic liquids (ILs) are organic salts composed of organic cations and organic/inorganic anions that remain in molten state at room temperature [1]. In comparison to the conventional volatile organic solvents, ILs are getting increasingly more and more attention due to their unique physiochemical properties such as high thermal and chemical stability, low volatility, non-flammability and high solvent capacity [2,3]. They are widely being used as solvents, reagents and catalysts for various applications in the field of chemical industry, chemical engineering, biotechnology and pharmaceutical industries [2,4–10]. Because of very low volatility, they do not pollute air and hence have gained reputation as environment-friendly harmless chemicals.

Despite numerous benefits that are associated with the uses of ILs, it is important to assess their negative impacts particularly on the aquatic environments as they are usually water-soluble and not easily biodegradable. They keep on accumulating in the environment and can easily reach the food chains of living organisms. In fact, several studies have documented the toxic effects of ILs in various organisms including bacteria, yeast, algae, *Hydra*, *Daphnia*, nematode, fish, plants and various mammalian cell lines [11–20]. The toxicity and the susceptibility to the ILs varied from organism to organism largely depending on the nature of the anions, cations (whether imidazolium, pyridinium or morpholinium) and the length of the alkyl side chains attached to the ILs [12,21–27]. For instance, imidazolium heterocyclic ring-based ILs are found to be more toxic than ILs with morpholinium ring, while the toxicity of ILs with a pyridinium ring is stronger than that of the imidazolium ring [28,29]. Also increasing the alkyl chain length on the imidazolium and pyridnium cations enhances their toxicity towards aquatic organisms [18,25].

Studies based on toxicity assays, microscopy experiments and molecular dynamic simulations, have demonstrated that ILs can induce cytotoxicity via various mechanisms that include disrupting cell membrane by penetrating the membrane or affecting cellular metabolism that results in cell death via necrosis or apoptosis [11–13]. However,

* Corresponding author.
E-mail addresses: mukhop@barc.gov.in (R. Mukhopadhyay), ag315@snu.edu.in (A. Gupta), sajal.ghosh@snu.edu.in (S.K. Ghosh).

https://doi.org/10.1016/j.bbamem.2019.183103
Received 18 July 2019; Received in revised form 25 September 2019; Accepted 10 October 2019
Available online 31 October 2019
0005-2736/

previous studies have been done with extremely higher concentrations (in the range 100 μM to 100 mM) of ionic liquids, which can lead to aberrant death of biological cells. These kind of conditions can give artefact results, thus a clear understanding of the defined molecular mechanism by which ILs mediate their cytotoxic effects remains largely unknown.

Any foreign molecule affecting a cellular organism inevitably has to interact with the cellular membrane of a eukaryotic cell. The effect of such an interaction can be transient or permanent depending on the type and strength of the interactions. As a result, the self-assembled structure and correspondingly, the physical properties of the membrane are expected to be perturbed momentarily or enduringly. To understand the molecular details of this perturbation, Evan et al. used a range of experimental techniques, atomic force microscopy (AFM), luminescence and quartz crystal microbalance. They have used imidazolium cation $[C_nmim]^+$ (n = 4, 6 and 8) and have shown that ILs with n = 6 and 8 make the lipid membrane more permeable compared to n = 4. At a concentration of 200 mM, these ILs completely destroy the lipid bilayer [30–32]. There were computational studies carried out by different groups [33,34]. In their works, Benedetto et al. have taken two different RTILs of same cation $[bmim]^+$ but with different anions [BF4] and [PF_6]. The study has revealed the favourable incorporation of $[bmim]^+$ into the lipid bilayer exhibiting a systematic thinning in the bilayer [36]. In their review papers, the results are well discussed [37–39]. The same group performed neutron reflectometry measurements on lipid bilayer of two different lipids; 1-palmitoyl-2-oleoyl-sn-glycero-3-phosphocholine (POPC) and 1,2-dimyristoyl-sn-glycero-3-phosphatidylcholine (DMPC). A shrinkage of the bilayer was observed and found to match very well with their simulation works [40]. There is a very recent work by Jeremy H. Lakey, that has discussed the recent advances in neutron reflectometry study in bio-membrane [41]. The structural effects of ILs on the model membrane observed in these studies indeed can influence the biochemical and biophysical activities of the membrane [42]. The consequences of this on the cellular communication, *exo*- and endocytosis processes, and functioning of trans- and peripheral membrane proteins may lead to cell death. It is to be noted that while the uncontrolled uses of these ILs raise the concern of cytotoxicity, the regulated and selective uses can bring us benefit in controlling the sickness caused by micro-organisms [9,28]. In the case of biological assays followed in many of the studies mentioned above, the concentrations of ILs used to investigate their effects on living organisms were in the range of mM. Further, in the case of biophysical approaches, synthetic lipid molecules have been used mostly as a mimic of the cellular membrane. In the present paper, a systematic approach has been taken to understand the effect of ILs on various mammalian cell lines and all the biological assays were performed at 1–25 μM concentration which are within the range of acceptable limits, to avoid artifacts or non-specific results. The lipids used in this work are liver lipid extracts (bovine) which are physiologically relevant model systems.

In the first step, various imidazolium-based ILs with varying chain lengths have been used to investigate their effect on cell survival. The cell viability assay along with the fluorescence-activated cell sorting (FACS) analysis and comet assay indicated cell death without any DNA damage or apoptosis. The result was found to be dependent on the strength of hydrophobicity of the used ILs. Further, out of various cell lines, human liver cancer cell lines have found to be most impaired. These liver cells, which showed maximum cell death in the presence of ILs were used for the atomic force microscopy measurements. The morphology of the cells treated with IL was found to have numerous pores in the cell membrane and a distinctly different morphology from that of the untreated cell. To study the effect at the molecular level, two biophysical approaches were taken where liver lipid extract was used to mimic the liver cell membrane. In the first approach, lipid monolayers formed at the air-water interface were used as a model cellular membrane and then the interaction of the IL with the lipid layer was investigated. In the second approach, unilamellar vesicles were used as a model membrane system and quasi-elastic neutron scattering (QENS) experiments were carried out to investigate effects of the IL on the dynamical behaviour of the lipids. QENS is one of the most suitable techniques to study dynamics of lipid bilayer and has been used recently on various lipid bilayer systems [43–51]. Being a scattering technique, it has an advantage over other conventional techniques like nuclear magnetic resonance (NMR), dielectric relaxation spectroscopy as it provides information on dynamics in spatial as well as in temporal domains. Lipid bilayers have a complex dynamical behaviour. Different motions such as vibrational, rotational, lateral, bending, thickness fluctuation, etc. of the lipid occur in a wide range of time and length scales. It is difficult to disentangle these motions from one set of experiment. QENS is very convenient to study the dynamics in nanoseconds to picoseconds time scale and has been employed to investigate the lateral and internal motion of lipids [26–34]. In the present system, the QENS measurements have shown that the IL molecules accelerate the lateral motion of the lipids in the unilamellar vesicles. This was quantified by the diffusion coefficient of the lipid molecules.

2. Materials and methods

2.1. Materials

All the ionic liquids 1-ethyl-3-methylimidazolium tetrafluoroborate ([EMIM][BF4]), 1-butyl-3-methylimidazolium tetrafluoroborate ([BMIM][BF4]), 1-methyl-3-octylimidazolium C([DMIM][BF4]), 1-ethyl-3-methylimidazolium chloride ([EMIM][BF4]), 1-methyl-3-octylimidazolium chloride ([OMIM][BF4]), 1-decyl-3-methylimidazolium chloride ([DMIM][BF4]) and propidium iodide were purchased from Sigma Aldrich (USA). The liver lipid extract (bovine) was purchased from Avanti Polar (USA) with the components PC:PE:PI:lysoPI:cholesterol:other lipids = 42:26:9:1:5:17 (weight%). LB Agar, triton X 100, EtBr, YPD Agar and RNase were purchased from Himedia (India). NaCl, KCl, EDTA were purchased from Fischer Scientific (USA). Sodium phosphate dibasic anhydrous, potassium phosphate, NaOH, tris base and H_2O_2 were purchased from Amresco (USA). Low melting agarose were purchased from Lonza (Switzerland). DMEM, FBS and trypsin were purchased from Gibco (USA). These chemicals were used without further purification. To prepare the aqueous solution of the ILs, de-ionized water (Millipore, resistivity ~18 MΩ cm, with pH~7.0) was used. For neutron scattering measurements, D_2O from Sigma Aldrich (USA) was used in place of H_2O. The molecular structures of all these ILs are shown in Fig. 1.

2.2. Cell viability assay

HepG2 (human liver cancer cell line), Huh7 (human liver cancer cell line), Huh7.5 (human liver cancer cell line), MCF-7 (human breast cancer cell line) and HCT116 (human colon cancer cell line) were purchased from American Type Culture Collection (ATCC) and National Centre for Cell Science (NCCS, Pune) and were used to test the effect of the ILs ([EMIM][BF4], [EMIM][BF4], [BMIM][BF4], [OMIM][BF4], [OMIM][BF4], [DMIM][BF4] and [DMIM][BF4]) at different concentrations (0, 0.1, 0.5, 1, 10, 25, 50 and 100 μM). Cells were seeded in 12 well plates at 0.05 million cells and ILs were added at different concentrations and cells were incubated for 48 h. Post 48 h, the cells were counted by hemocytometer to determine the number of viable cells.

To test bacterial cell viability, DH5α strain of *E. coli* cells were grown at 310 K until the optical density (OD) reached 0.6. Cells were diluted to 1:10000 dilution and treated with ILs [DMIM][BF4] (test sample), [BMIM][BF4] (as negative control) at different concentrations (0, 10, 25, 50 and 100 μM). Then the cell suspension was plated on LB agar plates and kept at 310 K in an incubator for overnight growth. Colonies were observed and counted manually.

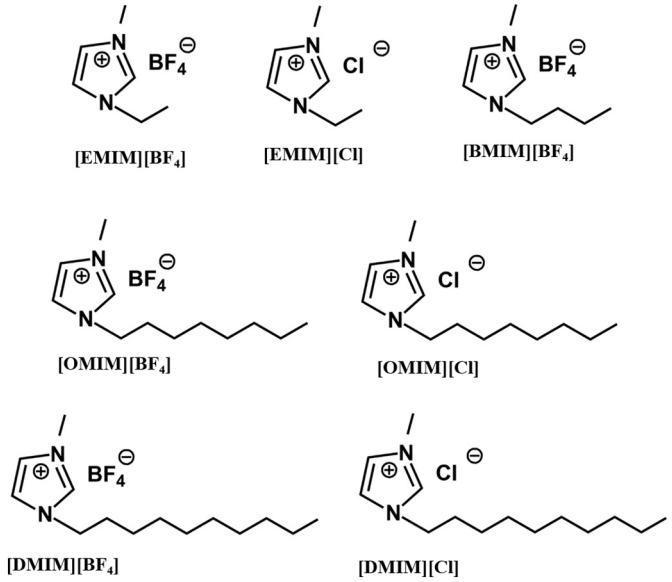

Fig. 1. Molecular structures of imidazolium-based room temperature ionic liquids (RTILs).

To determine the effect of ILs on yeast, *Saccharomyces cerevisiae* was grown in yeast extract peptone dextrose (YPD) media at 298 K until OD reached 0.6. We diluted this culture to 1:2000 and then treated it with ILs [DMIM][BF4] (test sample) or [BMIM][BF4] (negative control) at different concentrations (0, 10, 25, 50 and 100 μM) and plated on YPD plates. After 48 h at 298 K, the colonies were observed and counted manually.

2.3. Fluorescence-activated cell sorting (FACS) for cell cycle and cell death analysis

To examine the effects of ILs on cell cycle, FACS analysis was performed. Huh7.5 cells were seeded in 60 mm dishes in [DMIM][BF4] with serum media at 0.6 million cells/well. Cells were treated with 10 μM [DMIM][BF4] (test sample) and controls (untreated cells) and kept for further incubation for 24 or 48 h. Post incubation, cells were washed with 1X PBS (with 5 mM EDTA (pH 8)) followed by trypsinization. The cells were further re-suspended in 1X PBS and centrifuged at 2500 rpm for 5 min at 4 °C. Then cells were fixed for 2–3 h in chilled 70% ethanol with 5 mM EDTA. Fixed cells were further washed with 1X PBS followed by RNase treatment (10 μg, ml) for 30 min at room temperature. 10 μg/ml propidium iodide (PI) was added to these cells and incubated for 15 min in dark. Stained cells were then analyzed in Flow Cytometer BD FACS Aria™ III cell sorter for cell cycle analysis and apoptotic cells population.

2.4. Comet assay

To determine whether cells death due to ILs occur due to DNA damage, a comet assay was performed. 0.1 million Huh7.5 cells were seeded on a 35 mm plate and treated with either 20 μM H_2O_2 (DNA damaging compound) or 1 μM and 10 μM [DMIM][BF4] (test sample) or [BMIM][BF4] (as a negative control). Treated cells were incubated for 48 h and then trypsinized. 2×10^4 trypsinized cells (in 100 μl PBS) were mixed with 100 μl of 1% low melting agarose. 100 μl of this cell suspension was then poured on microscopic slide precoated with 1% low melting agarose. Slide was kept in lysis buffer (2.5 M NaCl, 100 mM EDTA, 10 mM Trizma base, 1% Triton X-100, 0.26 M NaOH, pH -10.0) overnight at 277 K. Further, these slides were placed in electrophoresis buffer (10 N NaOH, 200 mM EDTA, pH > 13) twice for 20 min and then electrophoresis was performed at 25 V, 400 mA for 30 min. Slides were rinsed once with de-ionized water and then stained with EtBr (2 μg/ml) for 20 min. Again, slides were rinsed with de-ionized water and then microscopy was performed using Nikon Ti fluorescence microscope.

2.5. Atomic force microscopy (AFM)

To study the effect of ILs on mammalian cells, AFM was performed. Huh7.5 cells were seeded on a coverslip at 0.1 million cells/well in 6 well plates. The cells were then treated with 10 μM [DMIM][BF4] and incubated for 48 h. Cells were then washed with 1X PBS and fixed using 2% glutaraldehyde (in PBS) for 15 min and further washed twice with MQ water and then dried using liquid nitrogen. The cells were air dried and taken on a glass cover slip. The atomic force microscope (AFM) (XE7, Park System) was used to visualize the topography of the cells treated with or without [DMIM][BF4]. A PPP-NCHR tip of force constant 40 N/m with the resonant frequency of 330 kHz was used for all the measurements (non-contact mode). In all cases, scan rate was 0.4 Hz in each measurements, a $40 \times 40\ \mu m^2$ area was scanned covering a total of 1024 × 1024 pixels.

2.6. Lipid monolayer

A Langmuir trough of size $55 \times 15 \times 0.5\ cm^3$ (Apex, India) with two Teflon barriers has been used to determine the interaction of the ILs with a liver lipid monolayer formed at air-water interface. Two methods were employed to quantify the interactions; the change in surface pressure and the surface pressure-area isotherms of the lipid monolayers with and without the ILs.

The stock solution of the lipid was prepared in chloroform with a final concentration of 0.5 mg/ml. Then, 125 μl of the stock solution was spread over the water surface by using a Hamilton micro syringe and waited for about 15 min for the complete evaporation of the solvent. For the time evolution of surface pressure, the monolayer of the lipid was compressed at a rate of 5 mm/min to a fixed pressure of 15 mN/m and then the aqueous solution of the respective ILs were injected in the water sub-phase at a distance of 4 cm away from the Wilhelmy balance. The time evolution of the surface pressure was then monitored. The relative change in the pressure was calculated by the equation, $\Delta\pi = \frac{\pi_f - \pi_0}{\pi_0}$, where π_0 and π_f are the initial and final surface pressure, respectively. For the surface pressure-area isotherm, [DMIM][BF4] was mixed into the chloroform solution of the lipid to achieve a composition of lipid: IL = 9:1 (mol:mol). After forming the monolayer of the mixture, the barriers were compressed at the same rate as above until the collapsed pressure of the monolayer was reached. The temperature was maintained at 293 K for all the measurements.

2.7. Preparation of unilamellar vesicles

Unilamellar vesicles (ULV) based on liver lipid were prepared using the extrusion method as described by us earlier [29–33]. Briefly, the liver lipid solution in chloroform was taken in a glass vial and chloroform was evaporated using the gentle stream of nitrogen gas to obtain lipid films. To remove the residual organic solvent, the lipid films were dried under vacuum for about 10 h at room temperature. Dry lipid films were suspended in the desired amount of D_2O at 310 K and taken through 3-freeze-thaw cycles by alternately placing the lipid suspension in a warm water bath (323*K*) and in a freezer (193 K). This lipid suspension was passed through a mini-extruder with a porous polycarbonate membrane (pore diameter ~100 nm) 21 times. During the extrusion process, the temperature of the extruder was kept at ~323 K. The stock solution of [DMIM][BF4] IL was prepared by dissolving [DMIM][BF4] in D_2O (5% (*w/w*)). For the neutron scattering measurements, the samples of liver lipid ULV were prepared without and with 17.5 mol% [DMIM][BF4]. This mixture was kept at 310 K for

about 4 h for equilibration and then used for experiments.

2.8. Quasi-elastic neutron scattering (QENS)

QENS experiments were carried out on liver lipid ULV in the absence and presence of 10 wt% [DMIM][BF4] at physiological temperature of 310 K using high energy resolution IRIS spectrometer [52] at the ISIS pulsed Neutron and Muon source at the Rutherford Appleton Laboratory, UK. We have used IRIS with a PG(002) analyzer that provides an energy resolution $\Delta E = 17$ μeV (full width at half-maximum) and an accessible range of energy transfer from -0.3 to $+1.0$ meV in the offset mode. The available *Q*-range in the chosen configuration was 0.4 to 1.8 $Å^{-1}$. Samples were placed in annular aluminium sample cans with 0.5 mm internal spacing such that the sample scattering is no > 10%, thereby minimizing multiple scattering effects. For reference, measurements were also carried out on pure D_2O at 310 K. The instrumental resolution was obtained by recording the QENS spectra from a standard vanadium sample. MANTID software [53] was used to perform standard data reduction.

3. Results and discussions

Pyridinium-based, ammonium-based and many other ILs have been reported to be toxic to living organisms [18,28,54]. Imidazolium based ILs, on the other hand, are preferred by the pharmaceutical industry, as the N-substituted imidazolium ring is predominantly present in many natural products and also in bioactive molecules in the human metabolism [55,56]. Imidazolium based ILs are amphiphilic in nature and the highly polar head part is beneficial for many biological interactions, as explained in previous studies [19,27,57]. Moreover, they are likely to be liquid at room temperature whereas the others are solid. Unfortunately, these ILs show much higher toxicity compared to many others. Many studies in the last decades have studied the various effects of this class of IL with biological system, however no complete understanding of their interactions at a molecular level has been attained. In the present study, we provide further insight into their effects on human cells.

3.1. Effect of ILs on necrosis dependent cell death in mammalian cells

To determine the effect of the ILs on mammalian cells, a cell survival assay was performed with various human cell lines. Mammalian cells were treated with the ILs and surviving cells were counted 48 h post treatment. Results showed that ILs with short carbon chains, [EMIM][BF4] (2-carbons) and [BMIM][BF4] (4-carbons), did not show any significant toxicity towards the cells (Fig. 2A). However, the ILs with chain lengths above 4-carbon showed increasing toxicity with increasing carbon chain length. [DMIM][BF4] with the 10-carbon chain length showed high toxicity towards human cells (Fig. 2A). There is no significant difference in results when the $BF4^-$ anion was replaced by Cl^-. Thus, the results show that higher carbon chain ILs has higher toxic effect on human cells.

Once established that the high carbon chain ILs are toxic for human cells, we wanted to determine whether this toxic effect is specific to human cells or whether these ILs can kill other kind of cells like bacteria and yeast. Results showed that under a similar concentration, none of the ILs inflicted any significant cell death in *E. coli* bacteria (Fig. 2B) or in yeast *Saccharomyces cerevisiae* (Fig. 2C).

In cell viability assay above, it has been shown that ILs with longer hydrocarbon chain have the most severe effects in killing human cells. Hence, in the following sections, the IL with highest chain [DMIM][BF4] has been used. To determine the effect of this IL on the cell cycle of human cells, Huh-7.5 cells were treated with the IL and cell cycle analysis was performed by FACS Results showed no change in the cell cycle pattern of Huh-7.5 cells on 24 or 48 h of treatment (Fig. 3A). Furthermore, to detect any damage on DNA of human cells, comet assay was performed. Huh-7.5 cells were treated with different concentrations of [BMIM][BF4], [DMIM][BF4] or H_2O_2 as a positive control. Results show that in the presence of H_2O_2 almost 70% of the cells indicated DNA damage, however under similar conditions, with IL, there was no significant increase in number of cells showing DNA damage (Fig. 3B). These results confirmed that [DMIM][BF4] specifically induces human cell death but does not cause cell cycle inhibition or DNA damage.

3.2. Effect of IL on cell morphology

There are very few reports using AFM to study the effects of ILs on biological cells. As mentioned earlier, Evans et al. observed an increased roughness in a model phospholipid bilayer membrane in the presence of an IL [30]. There is further scope to the application of this microscopic technique to obtain a direct pictorial presentation of IL-membrane interactions.

Since the long chain IL [DMIM][BF4] exhibited strongest effect on cell death, this molecule was used in the subsequent AFM study. For a direct visualization of the effect of IL on the surface morphology of the human cells, AFM was performed on Huh-7.5 cells. In a very recent publication, Benedetto et al. have used AFM to study the surface morphology and local elastic modulus of osteoblast cells [38]. The present study clearly shows that the surface morphology of the cell treated with the IL is modified compared to the untreated one (Fig. 4A and B). The corresponding height profiles for untreated and treated cells are shown in Fig. 4C and D, respectively. While the untreated cell shows a smooth height profile, the treated one shows a rough profile indicating an uneven surface. These images suggest that the IL probably causes the formation of micron size pores in the cellular membrane. Note that the AFM images cannot be used as a single data set to conclude unambiguously the formation of pores, as this technique only provides visual images related to a probable structural change in the membrane. In the present case, it has been shown in the biological assays above, that the effects of ILs are not related to DNA damage. In agreement with our previous study, live/death cell viability assay results show that a long chain IL at higher concentration destroys the bacterial cell membrane [54]. Hence, all these results indicate that the IL-induced cell death is most likely related to the damaged cellular membrane.

3.3. Effect of mixing IL with lipids

The cellular membrane is, predominantly, composed of two leaflets of self-assembled lipid monolayers [58,59]. Following the results above suggesting that mammalian cell death is linked with effects on the cellular membrane, a simple model system has been adopted here to provide the molecular description on the effect of the ILs on the self-assembled structures of lipid layer. As human liver cells have shown strongest effects, we chose a mimic of the cellular membrane using the liver lipid extract to prepare the lipid monolayer. This lipid layer is a self-assembled two-dimensional monolayer of molecules formed at the air-water interface where the head groups are in contact with water and the chains are projecting out in the air. This is an excellent model cell membrane system to investigate the interaction of foreign molecules, such as inorganic or organic salts [59–61], probable drug molecules, cholesterols [62], and proteins [63,64]. In the present study, this system is used to quantify the interaction of imidazolium-based ILs with liver lipids. At the initial surface pressure of 15 mN/m, 50 μM IL was injected into the water subphase and the corresponding pressure change was monitored over time. As a consequence of the insertion of these ILs into the lipid film, the in-plane pressure was expected to increase. The relative change of the pressure is shown in Fig. 5. There is no change in the pressure for the pure liver lipid but the change is evident with the addition of the ILs. The pressure change in the presence of ILs increases with time and reaches to a saturation value. The effect is very sensitive to the number of carbons in the hydrocarbon

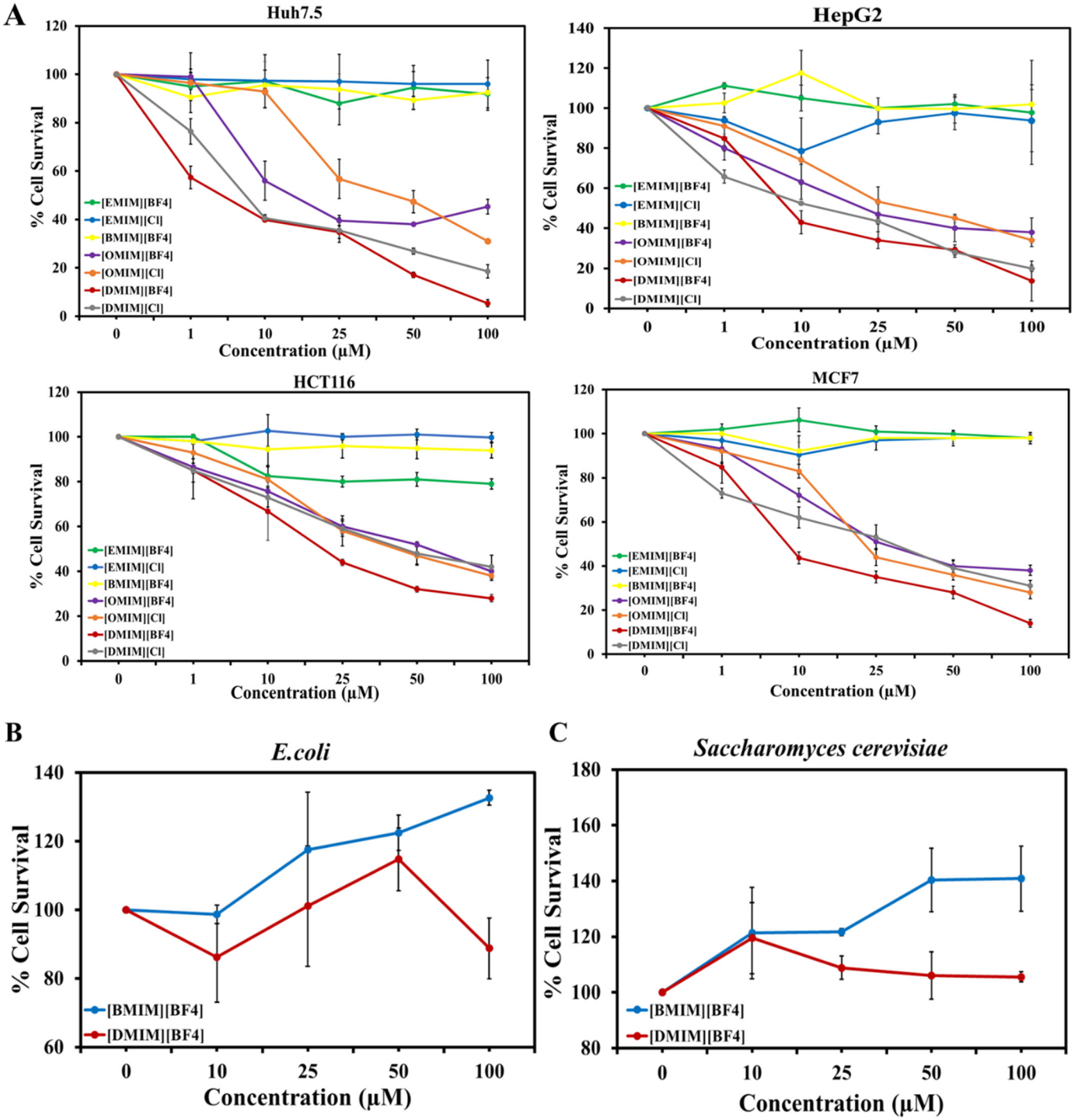

Fig. 2. Effect of ionic liquids on cell viability. (**A**) Several mammalian cell lines Huh7.5, HepG2, HCT116, MCF7 were treated with ionic liquids ([EMIM][BF4], [EMIM][Cl], [BMIM][BF4], [OMIM][BF4], [OMIM][Cl], [DMIM][BF4] and [DMIM][Cl]) at different concentrations (0, 1, 10, 25, 50, 100 μM). After 48 h of treatment with ionic liquids, cells were trypsinized and counted using hemocytometer. (**B**) To investigate the effect of ionic liquids on bacterial cells, DH5α *E. coli* strain was grown in incubator at 310 K.. Secondary culture was grown till O.D. reached to 0.6 and dilution of 1:10000 of bacterial cells were made and treated with ionic liquids [DMIM][BF4] (test sample), [BMIM][BF4] (as negative control) at different concentrations (0, 1, 10, 25, 50, 100 μM) and were plated on LB plates. After 12 h colonies were counted manually, and bar graph was plotted. (**C**) To further explore cell viability in yeast, *Saccharomyces cerevisiae* strain was taken. As absorbance reached 0.6, cells were diluted to 1:2000 and treated with [DMIM][BF4] (test sample), [BMIM][BF4] (as negative control) at different concentrations (0, 1, 10, 25, 50, 100 μM). Post treated cells were plated on YPD plates and kept at 298 K incubator for 48 h. Colonies obtained were counted manually. A value of 100% represents cell survival without any added ionic liquid. The corresponding changes in the presence of ionic liquids have been plotted with respect to this scale.

chains of the ILs; the maximum effect (~75%) is observed for the longest chain ([DMIM][BF4]) with 10 carbon atoms and the least effect (~5%) for the shortest chain ([EMIM][BF4] with two carbon atoms (Fig. 5).

As also evidenced in other measurements, only the effect of the longest chain IL, [DMIM][BF4] on the surface-pressure area isotherm of the lipid was characterized and the corresponding data are shown in Fig. 6A. The presence of 10 mol% of the IL in the mixture of the liver

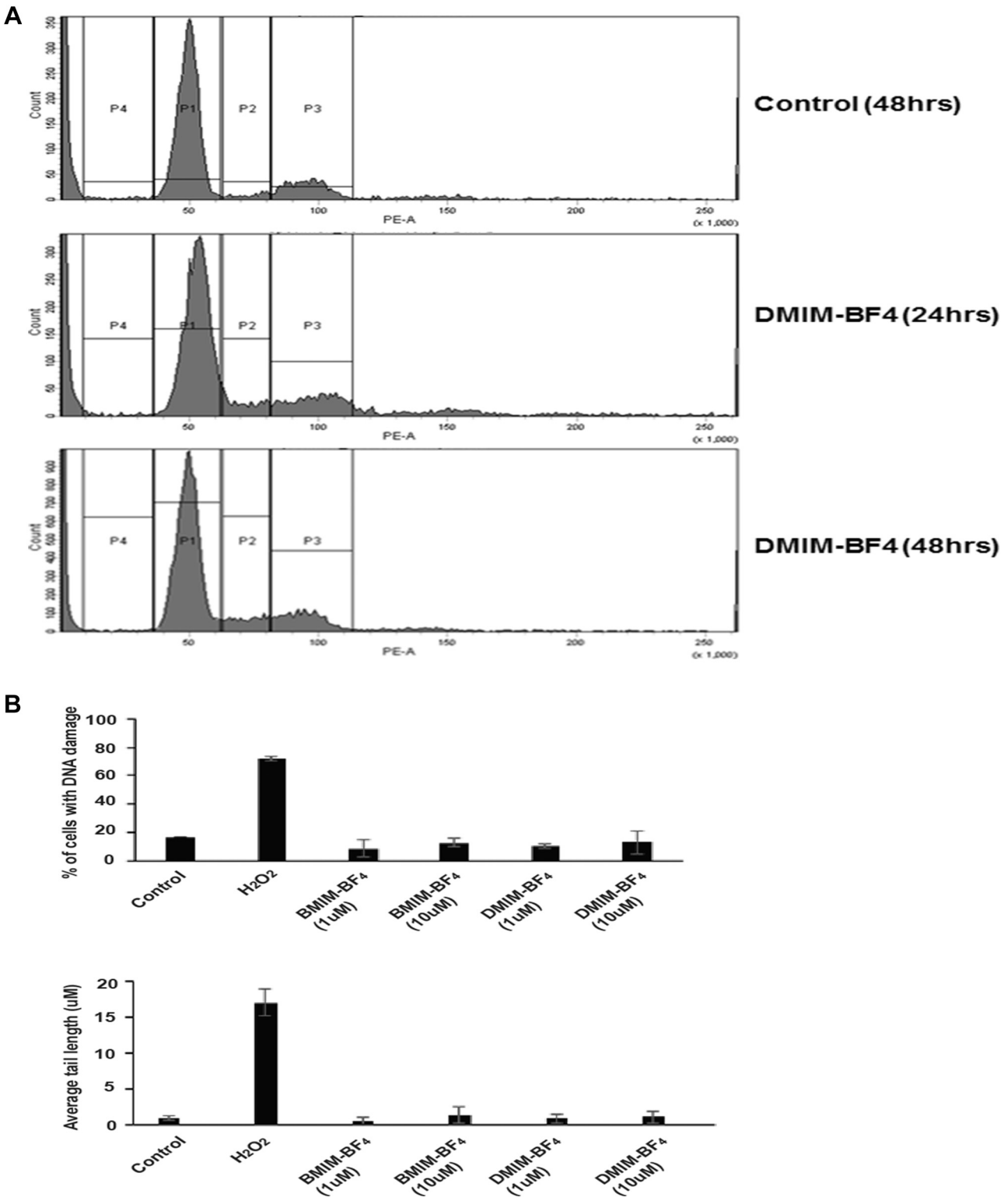

Fig. 3. Effect of ionic liquids on cell cycle and DNA damage. (**A**) The effect of ionic liquids on cell cycle FACS. Huh7.5 cells were treated with 10 μM [DMIM][BF4] (test sample) for 24 and 48 h. Post treatment cells were stained with PI stain for 30 min. Cells were analyzed for cell cycle analysis in Flow Cytometer BD FACS Aria™ III cell sorter. (**B**) Comet assay showing the effect of ionic liquid on apoptosis/necrosis. Huh7.5 cells were treated with 1 μM H_2O_2 (DNA damage positive control), 1 μM and 10 μM [DMIM][BF4] (test sample), 1 μM and 10 μM [BMIM][BF4] (as negative control) for 48 h. Further 2×10^4 cells were mixed with 1% low melting agarose and placed on microscopic slide precoated with 1% low melting agarose. Cells were lysed overnight, and electrophoresis was performed. Slides were stained with EtBr and visualized under Nikon fluorescence microscope.

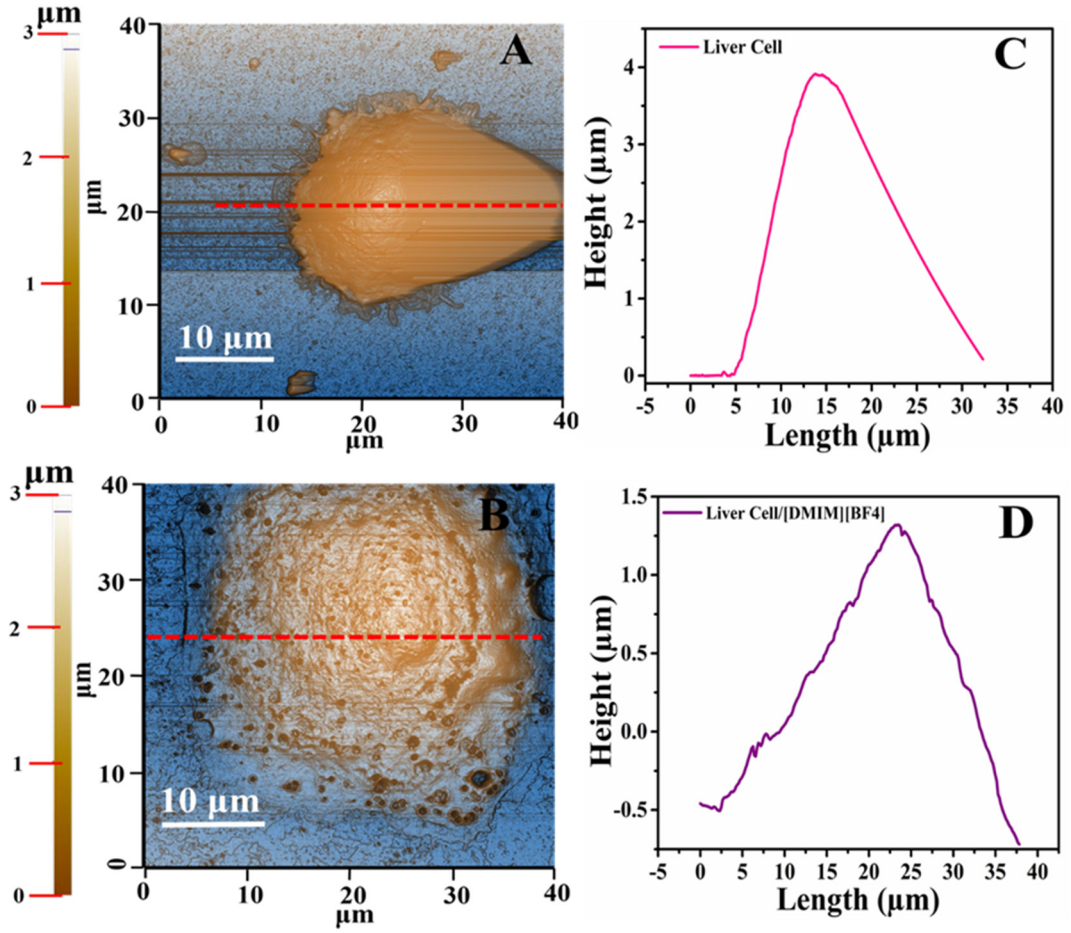

Fig. 4. AFM topography to determine effect of ionic liquid on cell membrane. To determine effect of ionic liquid on cell surface, Huh7.5 cells were grown on slides and treated with [DMIM][BF4].Cells were fixed with 2% glutaraldehyde, dried in liquid nitrogen and visualized under AFM. Untreated (A) and treated (B) with ionic liquid [DMIM][BF4]. The height profiles, (C) and (D), obtained from the line cuts (lines in A and B, respectively) exhibit the effect of the ionic liquid on the surface morphology of the cell.

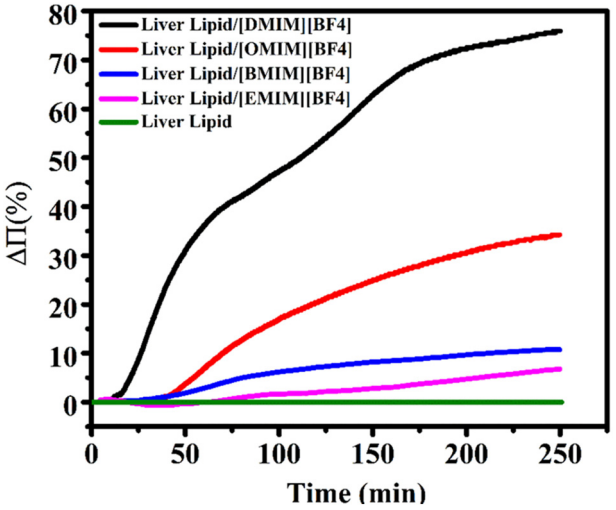

Fig. 5. Variation of surface pressure of liver lipid monolayers formed at the air-water interface. The imidazolium-based ionic liquids were injected in the water subphase at an initial surface pressure of 15 mN/m. The increment of surface pressure is found to be maximum for [DMIM][BF4] with the longest chain length (C10) and minimum for [EMIM][BF4] with the shortest chain length (C2).

lipid changes the characteristic isotherm of the lipids shifting the curve towards lower area-per molecule. Note that the mol% of IL is defined as $\frac{[IL]}{[Lipid]+[IL]} \times 100\%$, with [IL] and [Lipid] being the number of moles of IL and liver lipid, respectively. The mol% of an IL is defined as the number of moles of IL taken with respect to the number of moles of lipid in the chloroform solution. There is a possibility that some of the IL molecules may dissolve into the aqueous sub-phase and hence the actual mol% of the IL in equilibrated lipid monolayer may differ. An observation of shifting the curve for synthetic lipids has already been reported in Ref [59, 60]. The effect of the IL on the isotherm of the lipid is also evident as its presence changes the collapsed pressure to 42 mN/m from 30mN/m for liver lipid. Note that the IL itself is a surface active molecule as it shows its own characteristic isotherm (Fig. 6A). The presence of the IL in the lipid monolayer is expected to affect the physical properties of the membrane. The in-plane elasticity (E_s) of the lipid layer at constant temperature (T) is calculated using [59].

$$E_s = -A\left(\frac{\delta\pi}{\delta A}\right)_T \quad (1)$$

where A is the mean molecular area and π is the surface pressure. As shown in Fig. 6B, the in-plane elasticity of the lipid layer drops due to the presence of the IL and the effect is prominent at the higher surface pressure. It suggests that the IL mixes in the lipid layer and it becomes easy for the layer to compress. This result indicates that the well-packed lipid molecules in the layer have been relaxed by the presence of the IL. As reported by us earlier using synchrotron x-ray scattering measurements [58,59], such relaxation is due to more conformational

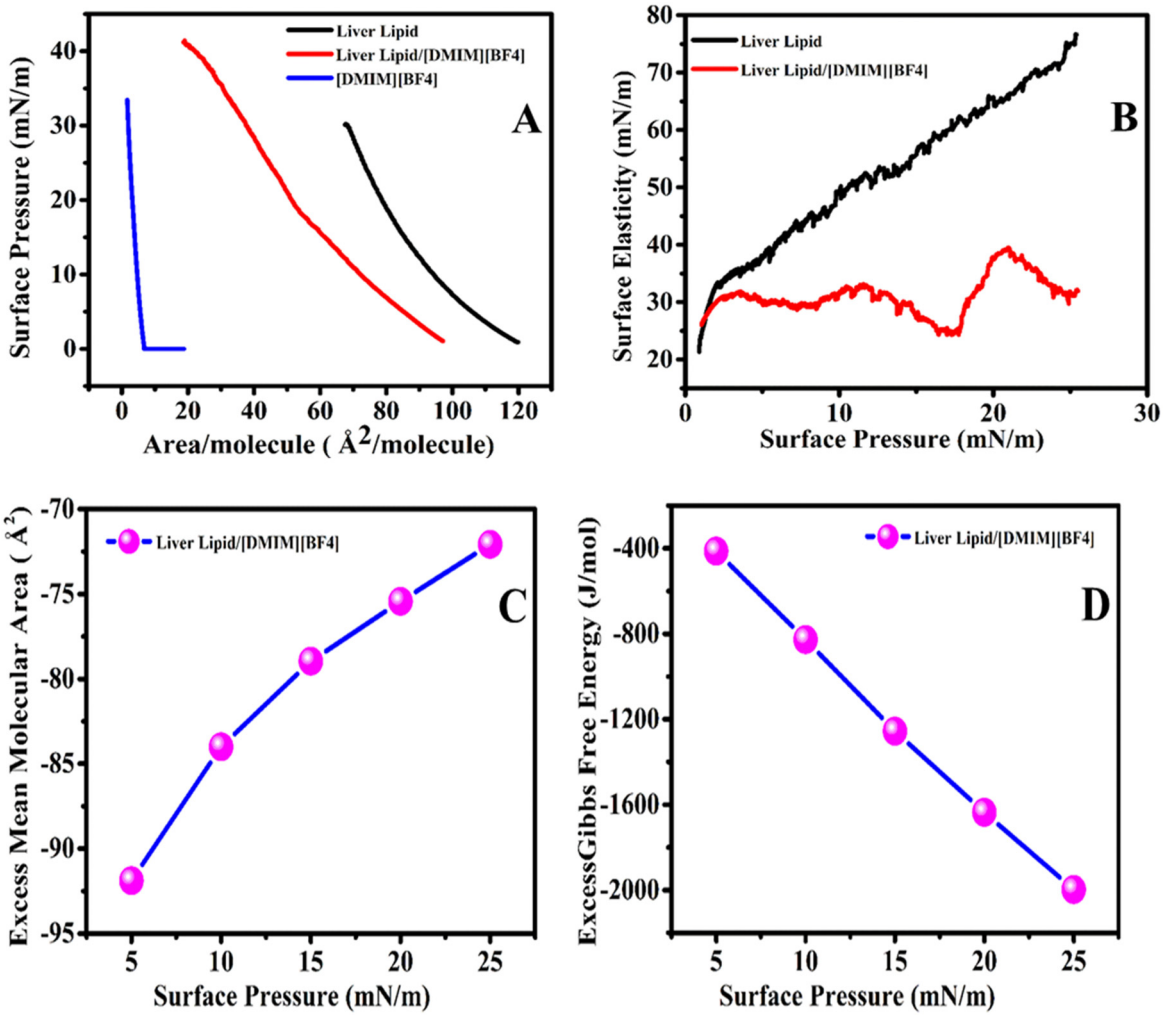

Fig. 6. Thermodynamic parameters of the interaction of ionic liquid (IL) [DMIM][BF4] with liver lipid monolayer formed at the air-water interface. (A) Area-surface pressure isotherms; (B) surface elasticity of the monolayer exhibiting the decrease in the elasticity at the presence of the IL, (C) excess mean molecular area at the presence of the IL which increases with increasing the surface pressure and (D) the Gibb's free energy of interaction which decreases with increasing surface pressure.

disordered organization of the hydrocarbon chains of the lipids. Such re-arrangement of molecules and hence the structural changes in the membrane might have adverse effect on its function. The mixing of the IL molecules is further quantified by calculating the excess mean molecular area (ΔA) as shown in Fig. 6C. This is calculated from the isotherm data using [65],

$$\Delta A = A_{lipid-IL} - (M_{lipid}A_{lipid} + M_{IL}A_{IL}), \quad (2)$$

where, M_{lipid}, M_{IL} and A_{lipid}, A_{IL} are the molar fractions and areas of liver lipid and the IL, respectively. While $\Delta A = 0$ siginifies an ideal mixing of these two components, the negative value corresponds to an attractive interaction between the lipid and IL molecules. The preferred attractive interaction is evident from the negative value of ΔA as shown in the Fig. 6C. However, the value becomes less negative at higher surface pressure as it becomes hard for any foreign molecule to penetrate into the well packed lipid layer. From this excess mean molecular area, one could calculate the excess Gibbs free energy (ΔG), which is the difference between the real (non-ideal) and ideal mixing of components. The ΔG is calculated using the following equation [66],

$$\Delta G = \int_0^{\pi} \{A_{lipid-IL} - (M_{lipid}A_{lipid} + M_{IL}A_{IL})\}d\pi. \quad (3)$$

The negative values (ΔG) as plotted in Fig. 6D exhibit a spontaneous interaction between the lipids and IL molecules.

To gain further insights of the physical behaviour of the lipid molecules in the presence of the IL, the dynamics of lipid molecules are measured as described in the following section.

3.4. Effect of the IL towards microscopic dynamics of the lipids

QENS is an excellent technique to probe the dynamics in nano- to pico-second time scales that provide the lateral and internal motion of lipids in unilamellar vesicles. In our previous work, this technique was successfully used for understanding the nanoscopic dynamics and phase behaviour of a model membrane formed by DMPC [44]. In the present work, QENS has been used to a more biologically relevant lipid system extracted from bovine liver.

The pressure area isotherm measurements indicate that incorporation of IL enhances the elasticity of the membrane. The molecular motions of the lipid were investigated using QENS on liver lipid ULV in the presence and absence of the long chain IL [DMIM[BF4]. Given the much smaller neutron scattering cross section of deuterium with respect to hydrogen, D_2O was used as a solvent to minimize its contribution to the QENS data and thereby enhance the relative contribution from the liver lipid membrane. Typical observed QENS spectra for liver lipid ULV solution and D_2O at 310 K at a typical Q value of 1.4 $Å^{-1}$ are shown in Fig. 7A. The solvent contribution is scaled by the volume fraction of the solvent in the ULV solution and subtracted from those of the liver lipid ULV solution, following the procedure described in the literature [44]. Subtracted QENS spectra, which correspond solely to the contribution

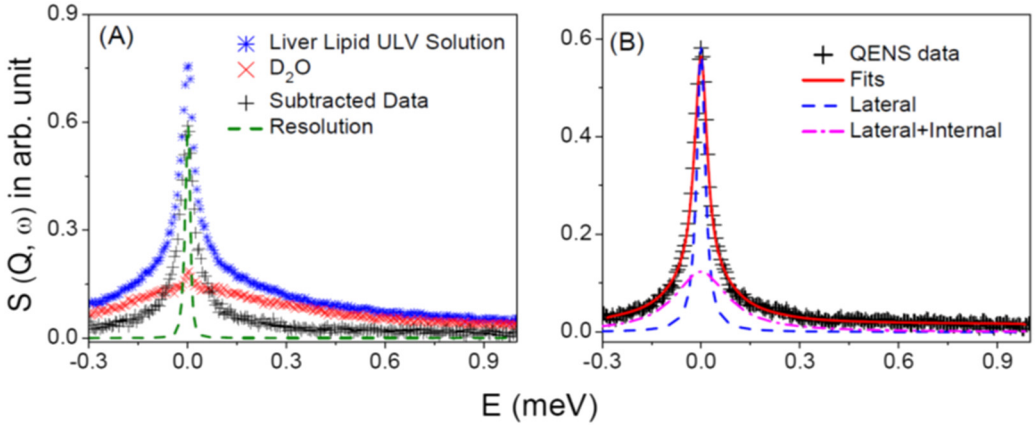

Fig. 7. (A) Typical measured QENS spectra for liver lipid ULV solution, D_2O at Q = 1.4 Å^{-1} Contribution from the liver lipid membrane (after subtracting the contribution of D_2O) is also shown. Instrument resolution as measured using standard vanadium is shown by dashed line. (B) Typical fitted QENS spectra from liver lipid membrane at $Q = 1.4$ Å^{-1}. Components correspond to lateral and internal motions are shown by dashed and dashed –dotted lines.

from the liver lipid membrane are shown in Fig. 7A. The instrumental resolution, as measured using a standard vanadium sample is shown by the dashed line in the figure. For comparison, data are normalised to the peak amplitude of the subtracted QENS spectra. Significant quasielastic (QE) broadening is observed for the liver lipid membrane indicating the presence of stochastic motion of the lipid molecules.

QENS investigates the molecular motions on the time scales from nanoseconds to picoseconds and length scale of Angstroms to few nanometers. On this length and time scales, lipid molecules can undergo two different kinds of motions: (i) lateral, a motion in which the whole lipid molecules diffuse within the leaflet and (ii) a relatively faster internal motion. Thus, the resultant scattering law for a lipid membrane will be the convolution of the scattering laws corresponding to lateral and internal motions and can be written as [46–50],

$$S(Q,\omega) = [A(Q)L_{lat}(\Gamma_{lat},\omega) + (1 - A(Q))L_{tot}(\Gamma_{lat} + \Gamma_{\text{int}},\omega)] \quad (4)$$

where, Γ_{lat} and Γ_{int} are the half-width-at-half-maximum (HWHM) of the Lorentzian functions corresponding to lateral and internal motions of the lipid. $A(Q)$ is elastic incoherent structure factor (EISF) of the localised internal motion. DAVE software [67] developed at the NIST Centre for Neutron Research has been used for the QENS data analysis. It is found that the scattering law given in Eq. (4) describes the observed QENS data well IL for the entire Q range.

A typical fit of the QENS data for the liver lipid membrane at Q = 1.4 Å^{-1} is shown in Fig. 7B.

The components corresponding to the lateral and internal motions are also indicated in the figure. The lateral motion of the lipids is of principal interest since it plays an important role in various physiologically relevant membrane processes, such as cell signalling, membrane trafficking, location and activity of membrane proteins, cell recognition, and so on. The HWHM of the Lorentzian functions corresponding to the lateral motion, Γ_{lat} for liver lipid with and without [DMIM][BF4] at 310 K are shown in Fig. 8. It is found that for both systems, Γ_{lat} increases linearly with Q^2 passing through the origin, which indicates that the lateral motion of lipid molecules undergo continuous diffusion, described by Fick's law $\Gamma_{lat} = D_{lat}Q^2$ as shown by the solid lines in Fig. 8. It is clear that, addition of [DMIM][BF4] increases the HWHM values, indicating enhancement in/faster lateral diffusion. Results are consistent with the earlier studies [27,34] which indicate that the incorporation of ILs enhances the fluidity of the membrane. The obtained lateral diffusion coefficients, D_{lat}, for pure liver lipid and with [DMIM][BF4] at 310 K are found to be $11.6 \pm 0.3 \times 10^{-7}$ cm^2/s and $13.4 \pm 0.4 \times 10^{-7}$ cm^2/s respectively. Our measurements suggest that incorporation of [DMIM][BF4] accelerates the lateral motion of the lipids. The accelerated lateral motion could be related to the relaxed and disordered chain configuration of the lipids indicated by the pressure-area isotherms discussed in previous section. The faster lateral motion of lipid molecules is a significant result, which indicates that incorporation of IL affects the dynamical behaviour of the lipid membrane.

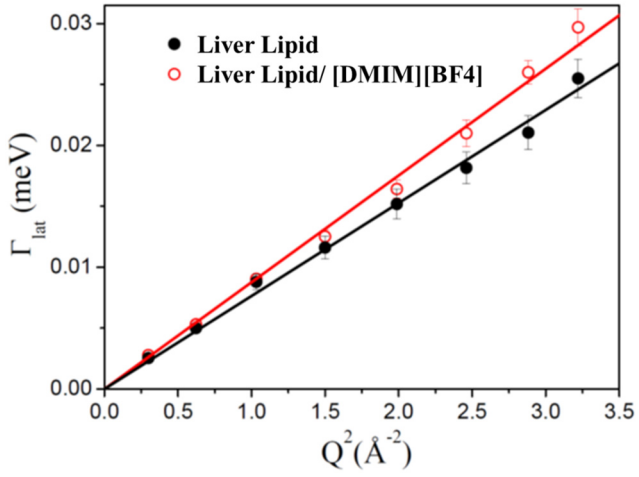

Fig. 8. Variation of HWHM's of Lorentzian function corresponding to the lateral motion for liver lipid in absence and presence of [DMIM][BF4] at 310 K. Solid lines are the fits assuming Fick's law of diffusion.

Cell membrane is a heterogeneous mixture of various lipids, proteins and other small molecules such as carbohydrates, cholesterols and it separates the extracellular space, outside of the cell, from the cytosol inside the cell. For cell membranes to function properly, they must maintain an appropriate level of fluidity, to allow movement of proteins and lipids within the membrane without compromising membrane integrity and allowing substances to leak in or out of the cell. Fluidity is very important for various physiological functions such as cell signalling, permeability, membrane fusion, cell division, exocytosis and endocytosis processes [68,69]. The extent of molecular motions within a lipid bilayer is referred to as fluidity of the membrane. Any perturbation in the membrane structure or dynamics caused by the foreign molecules may affect the stability of the cells. It is evident from the present studies that at the presence of ILs, the elastic nature of the lipid membrane changes which is a result of altered structure of the membrane. Further, dynamics of the lipid molecules get enhanced. This can be explained based on the interaction between IL and lipid membrane. Possibly, the ILs get absorbed first on the lipid membrane due to electrostatic interaction. Then, the hydrophobic part inserts into the hydrocarbon chain region of the membrane. This hydrophobic interaction enhances upon increasing the chain length of an IL as such an insertion makes the lipid chain configurationally disordered (indicated by higher fluidity in QENS measurements).

Any foreign molecule that affects a living organism has to encounter the outer boundary of the organism. Depending on the chemical

composition and physical properties of the surrounding layer, the effect may be different. As is observed in the biological assays, mammalian cells are prone to adverse effects from ILs compared to bacteria and yeast, owing to the different chemical composition of their interacting outer boundary [66,67]. *E. coli* is a gram-negative bacterium, which has peptidoglycan layer (7–8 nm) between its outer and inner membrane acting as a cell wall [68,69]. This peptidoglycan layer is made up of sugar (β-(1,4) linked *N*-acetylglucosamine (NAG) and *N*-acetylmuramic acid (NAM)) and amino acids. Yeast has a cell wall (70–100 nm thick) made up of polysaccharides (beta-glucan and mannan sugar polymers), proteins, lipids and chitins [35,70]. These structures provide protection to the cell membranes of both bacteria and yeast. In contrast, mammalian cells lack such a protective structure for the cell membrane, which is composed mainly of PC, PE, PI and other lipids, cholesterol and different membrane proteins [71,72]. Thus, when exposed to ILs, mammalian cells show drastic effects while no significant effect is observed on *E. coli* and *S. cerevisiae* cells. To explain in more detail why the response is different for mammalian cells, more systematic investigations are needed. Note that, even though the bio-assays and AFM study have indicated the mammalian cell death is related to the cellular membrane, it is not unambiguously conclusive that it is related to the altered physical properties of lipid bilayer only. Other components (transmembrane proteins, etc.) of cellular membrane may also be a target of these molecules. For example, the proteins that form ion channels may have modified structure after interacting with these molecules. In other case, simple adsorption of these molecules on the membrane surface may change the polarity of the membrane and hence the function of these channels. A more finely designed controlled experiments may shed lights on these issues in future.

In the case of antimicrobial peptides, it is reported that these peptides work as antibiotics, they kill the bacteria by forming pores in the cellular membrane. However, there is a minimum quantity of the peptide required in forming such a pore, as observed in model membrane systems [73,74]. The work reported by Sharma et al. [48] has shown that at very low concentration of these peptides, there is a considerable change in the lipid phase behaviour. Even at low concentration, these molecules can disrupt the lipid organization in the membrane, and as a consequence, the dynamics of the membrane alters. At the measured concentration of ILs in the present study, such a modified organization and dynamics of lipids are observed. At the same time, the AFM images have indicated the formation of pores in liver cell. It would be an interesting aspect to further investigate if the ILs form such a physical pore in the model membrane at high concentrations. One could either perform permeability measurements in vesicle systems or high resolution grazing incidence x-ray scattering study on lipid multilayer, which may be the subject of future study.

4. Conclusions

In this article, imidazolium-based ionic liquids (ILs) have been used to investigate their effects on various mammalian cells. The studies on the cell cycle and cell death indicate that the effect is strongly depended on the hydrophobic strength of the ILs. The ILs with > 4-hydrocarbons in their chain show increasingly high toxicity to human cells. Interestingly, in the physiological range of concentrations of these ILs, there are no significant effects on *E-Coli* bacteria and *Saccharomyces cerevisiae* yeast. Further, these ILs do not cause any cell cycle inhibitions or DNA damage in mammalian cells. **T**he cell death is observed to be related to the perturbed organization of the lipid molecules in the cellular membrane. To understand the molecular mechanism of such effects model membrane systems have been studied. In case of lipid monolayers formed at the air-water interface, the interaction of the ILs was thermodynamically stable, leading to changes in the physical structure and properties of the layer. The lipid molecules in the doubled-layered unilamellar vesicles have been found to enhance their dynamics in the presence of the ILs. It is found that the hydrophobic chains of the ILs go into the cellular membrane and introduce changes in the self-assembled structure and in the in-plane lateral motion. Such deviations in the natural structure and dynamics of cellular membrane might be the cause of a cell to die.

Even though this article describes a possible mechanism of mammalian cell death related to the reorganization of lipid molecules in the cellular membrane, the interaction of ILs with other components of membrane such as peripheral and integral membrane proteins should not be ignored. Hence, to find out the exact mechanism of toxicity of ILs more systematic investigations are to be done.

Transparency document

The Transparency document associated with this article can be found, in online version.

Declaration of competing interest

The authors declare that they have no conflicts of interest with the contents of this article.

Acknowledgements

KB thanks University Grant Commission (UGC), India and SM thanks Department of Science and Technology (DST), India for INSPIRE fellowship. AG is IYBA (Innovative Young Biotechnologist Award), fellow. S. K. G acknowledges the financial support received from UGC-DAE CSR (Mumbai Centre), India. R. M would like to thank the Department of Atomic Energy, India, for the award of Raja Ramanna Fellowship. We are thankful to Mr. Yogesh Yadav for his help in taking AFM images.

References

[1] T. Welton, Ionic liquids: a brief history, Biophys. Rev. 10 (2018) 691–706.
[2] D.D. Patel, J.M. Lee, Applications of ionic liquids, Chem. Rec. 12 (2012) 329–355.
[3] R. Sheldon, Catalytic reactions in ionic liquids, Chem. Commun. (2001) 2399–2407.
[4] H. Zhao, S. Xia, P. Ma, Use of ionic liquids as 'green' solvents for extractions, J. Chem. Technol. Biotechnol. 80 (2005) 1089–1096.
[5] W.L. Hough, M. Smiglak, H. Rodríguez, R.P. Swatloski, S.K. Spear, D.T. Daly, J. Pernak, J.E. Grisel, R.D. Carliss, M.D. Soutullo, The third evolution of ionic liquids: active pharmaceutical ingredients, New J. Chem. 31 (2007) 1429–1436.
[6] N.V. Plechkova, K.R. Seddon, Applications of ionic liquids in the chemical industry, Chem. Soc. Rev. 37 (2008) 123–150.
[7] M.S. Rajabi, M. Moniruzzaman, M.A. Bustam, M. Lotfi, Recent advances of ionic liquids in extarction of biologically active compounds: a review, Am. J. Chem. 5 (2015) 7–12.
[8] J. Xiao, G. Chen, N. Li, Ionic liquid solutions as a green tool for the extraction and isolation of natural products, Molecules 23 (2018) 1765.
[9] J. Pernak, K. Sobaszkiewicz, I. Mirska, Anti-microbial activities of ionic liquids, Green Chem. 5 (2003) 52–56.
[10] K.S. Egorova, E.G. Gordeev, V.P. Ananikov, Biological activity of ionic liquids and their application in pharmaceutics and medicine, Chem. Rev. 117 (2017) 7132–7189.
[11] S.-M. Lee, W.-J. Chang, A.-R. Choi, Y.-M. Koo, Influence of ionic liquids on the growth ofEscherichia coli, Korean J. Chem. Eng. 22 (2005) 687–690.
[12] S.P. Costa, P.C. Pinto, M.L.M. Saraiva, F.R. Rocha, J.R. Santos, R.T. Monteiro, The aquatic impact of ionic liquids on freshwater organisms, Chemosphere 139 (2015) 288–294.
[13] R.J. Bernot, M.A. Brueseke, M.A. Evans-White, G.A. Lamberti, Acute and chronic toxicity of imidazolium-based ionic liquids on Daphnia magna, Environ. Toxicol. Chem. 24 (2005) 87–92.
[14] C. Pretti, C. Chiappe, D. Pieraccini, M. Gregori, F. Abramo, G. Monni, L. Intorre, Acute toxicity of ionic liquids to the zebrafish (Danio rerio), Green Chem. 8 (2006) 238–240.
[15] R.F. Frade, A. Matias, L.C. Branco, C.A. Afonso, C.M. Duarte, Effect of ionic liquids on human colon carcinoma HT-29 and CaCo-2 cell lines, Green Chem. 9 (2007) 873–877.
[16] P. Stepnowski, A. Skladanowski, A. Ludwiczak, E. Laczyńska, Evaluating the cytotoxicity of ionic liquids using human cell line HeLa, Hum. Exp. Toxicol. 23 (2004) 513–517.
[17] M.C. Bubalo, K. Radošević, I.R. Redovniković, I. Slivac, V.G. Srček, Toxicity mechanisms of ionic liquids, Arch. Ind. Hyg. Toxicol. 68 (2017) 171–179.
[18] T.P.T. Pham, C.-W. Cho, Y.-S. Yun, Environmental fate and toxicity of ionic liquids: a review, Water Res. 44 (2010) 352–372.

[19] L. Carson, P.K. Chau, M.J. Earle, M.A. Gilea, B.F. Gilmore, S.P. Gorman, M.T. McCann, K.R. Seddon, Antibiofilm activities of 1-alkyl-3-methylimidazolium chloride ionic liquids, Green Chem. 11 (2009) 492–497.
[20] C. Zhang, S. Malhotra, A. Francis, Toxicity of ionic liquids to Clostridium sp. and effects on uranium biosorption, J. Hazard. Mater. 264 (2014) 246–253.
[21] J. Ranke, K. Mölter, F. Stock, U. Bottin-Weber, J. Poczobutt, J. Hoffmann, B. Ondruschka, J. Filser, B. Jastorff, Biological effects of imidazolium ionic liquids with varying chain lengths in acute Vibrio fischeri and WST-1 cell viability assays, Ecotoxicol. Environ. Saf. 58 (2004) 396–404.
[22] C. Samorì, A. Pasteris, P. Galletti, E. Tagliavini, Acute toxicity of oxygenated and nonoxygenated imidazolium-based ionic liquids to Daphnia magna and Vibrio fischeri, Environ. Toxicol. Chem. 26 (2007) 2379–2382.
[23] S. Stolte, M. Matzke, J. Arning, A. Böschen, W.-R. Pitner, U. Welz-Biermann, B. Jastorff, J. Ranke, Effects of different head groups and functionalised side chains on the aquatic toxicity of ionic liquids, Green Chem. 9 (2007) 1170–1179.
[24] R.F. Frade, C.A. Afonso, Impact of ionic liquids in environment and humans: an overview, Hum. Exp. Toxicol. 29 (2010) 1038–1054.
[25] Y. Xia, D. Liu, Y. Dong, J. Chen, H. Liu, Effect of ionic liquids with different cations and anions on photosystem and cell structure of Scenedesmus obliquus, Chemosphere 195 (2018) 437–447.
[26] S. Mitra, D. Ray, G. Bhattacharya, R. Gupta, D. Sen, V. Aswal, S. Ghosh, Probing the effect of a room temperature ionic liquid on phospholipid membranes in multilamellar vesicles, Eur. Biophys. J. 48 (2019) 119–129.
[27] K. Rawat, H. Bohidar, Universal charge quenching and stability of proteins in 1-methyl-3-alkyl (hexyl/octyl) imidazolium chloride ionic liquid solutions, J. Phys. Chem. B 116 (2012) 11065–11074.
[28] K.M. Docherty, C.F. Kulpa Jr., Toxicity and antimicrobial activity of imidazolium and pyridinium ionic liquids, Green Chem. 7 (2005) 185–189.
[29] Y. Yu, Y. Nie, Toxicity and antimicrobial activities of ionic liquids with halogen anion, J. Environ. Prot. 2 (2011) 298.
[30] K. Evans, Supported phospholipid bilayer interaction with components found in typical room-temperature ionic liquids–a QCM-D and AFM study, Int. J. Mol. Sci. 9 (2008) 498–511.
[31] K.O. Evans, Room-temperature ionic liquid cations act as short-chain surfactants and disintegrate a phospholipid bilayer, Colloids Surf. A Physicochem. Eng. Asp. 274 (2006) 11–17.
[32] K.O. Evans, Supported phospholipid membrane interactions with 1-butyl-3-methylimidazolium chloride, J. Phys. Chem. B 112 (2008) 8558–8562.
[33] S. Cromie, M. Del Popolo, P. Ballone, Interaction of room temperature ionic liquid solutions with a cholesterol bilayer, J. Phys. Chem. B 113 (2009) 11642–11648.
[34] R.J. Bingham, P. Ballone, Computational study of room-temperature ionic liquids interacting with a POPC phospholipid bilayer, J. Phys. Chem. B 116 (2012) 11205–11216.
[35] C.E. Ballou, Yeast cell wall and cell surface, Cold Spring Harbor Monograph Archive, 11 1982, pp. 335–360.
[36] A. Benedetto, R.J. Bingham, P. Ballone, Structure and dynamics of POPC bilayers in water solutions of room temperature ionic liquids, J. Chem. Phys. 142 (2015) (03B622_621).
[37] A. Benedetto, Room-temperature ionic liquids meet bio-membranes: the state-of-the-art, Biophys. Rev. 9 (2017) 309–320.
[38] A. Benedetto, P. Ballone, Room-temperature ionic liquids and biomembranes: setting the stage for applications in pharmacology, biomedicine, and bionanotechnology, Langmuir 34 (2018) 9579–9597.
[39] A. Benedetto, P. Ballone, Room temperature ionic liquids meet biomolecules: a microscopic view of structure and dynamics, ACS Sustain. Chem. Eng. 4 (2015) 392–412.
[40] A. Benedetto, F. Heinrich, M.A. Gonzalez, G. Fragneto, E. Watkins, P. Ballone, Structure and stability of phospholipid bilayers hydrated by a room-temperature ionic liquid/water solution: a neutron reflectometry study, J. Phys. Chem. B 118 (2014) 12192–12206.
[41] J.H. Lakey, Recent advances in neutron reflectivity studies of biological membranes, Curr. Opin. Colloid Interface Sci. 42 (2019) 33–40.
[42] J.E. Darnell, H.F. Lodish, D. Baltimore, Molecular Cell Biology, Scientific American Books, New York, 1990.
[43] P. Dubey, H. Srinivasan, V. Sharma, S. Mitra, V.G. Sakai, R. Mukhopadhyay, Dynamical transitions and diffusion mechanism in DODAB bilayer, Sci. Rep. 8 (2018) 1862.
[44] V. Sharma, S. Ghosh, P. Mandal, T. Yamada, K. Shibata, S. Mitra, R. Mukhopadhyay, Effects of ionic liquids on the nanoscopic dynamics and phase behaviour of a phosphatidylcholine membrane, Soft Matter 13 (2017) 8969–8979.
[45] S. Busch, C. Smuda, L.C. Pardo, T. Unruh, Molecular mechanism of long-range diffusion in phospholipid membranes studied by quasielastic neutron scattering, J. Am. Chem. Soc. 132 (2010) 3232–3233.
[46] V. Sharma, E. Mamontov, D. Anunciado, H. O'Neill, V. Urban, Nanoscopic dynamics of phospholipid in unilamellar vesicles: effect of gel to fluid phase transition, J. Phys. Chem. B 119 (2015) 4460–4470.
[47] V.K. Sharma, E. Mamontov, D.B. Anunciado, H. O'Neill, V.S. Urban, Effect of antimicrobial peptide on the dynamics of phosphocholine membrane: role of cholesterol and physical state of bilayer, Soft Matter 11 (2015) 6755–6767.
[48] V. Sharma, E. Mamontov, M. Tyagi, S. Qian, D. Rai, V. Urban, Dynamical and phase behavior of a phospholipid membrane altered by an antimicrobial peptide at low concentration, J. Phys. Chem. Lett. 7 (2016) 2394–2401.
[49] V. Sharma, E. Mamontov, M. Tyagi, V. Urban, Effect of α-tocopherol on the microscopic dynamics of dimyristoylphosphatidylcholine membrane, J. Phys. Chem. B 120 (2015) 154–163.
[50] V. Sharma, E. Mamontov, M. Ohl, M. Tyagi, Incorporation of aspirin modulates the dynamical and phase behavior of the phospholipid membrane, Phys. Chem. Chem. Phys. 19 (2017) 2514–2524.
[51] V. Sharma, R. Mukhopadhyay, Deciphering interactions of ionic liquids with biomembrane, Biophys. Rev. 10 (2018) 721–734.
[52] C. Carlile, M.A. Adams, The design of the IRIS inelastic neutron spectrometer and improvements to its analysers, Phys. B Condens. Matter 182 (1992) 431–440.
[53] J. Taylor, O. Arnold, J. Bilheaux, A. Buts, S. Campbell, M. Doucet, N. Draper, R. Fowler, M. Gigg, V. Lynch, Mantid, a high performance framework for reduction and analysis of neutron scattering data, APS Meeting Abstracts, 2012.
[54] D. Zhao, Y. Liao, Z. Zhang, Toxicity of ionic liquids, Clean–Soil, Air, Water 35 (2007) 42–48.
[55] D. Wang, C. Richter, A. Rühling, S. Hüwel, F. Glorius, H.-J. Galla, Anti-tumor activity and cytotoxicity in vitro of novel 4, 5-dialkylimidazolium surfactants, Biochem. Biophys. Res. Commun. 467 (2015) 1033–1038.
[56] D. Wang, D.H. de Jong, A. Rühling, V. Lesch, K. Shimizu, S. Wulff, A. Heuer, F. Glorius, H.-J. Galla, Imidazolium-based lipid analogues and their interaction with phosphatidylcholine membranes, Langmuir 32 (2016) 12579–12592.
[57] C. Samorì, D. Malferrari, P. Valbonesi, A. Montecavalli, F. Moretti, P. Galletti, G. Sartor, E. Tagliavini, E. Fabbri, A. Pasteris, Introduction of oxygenated side chain into imidazolium ionic liquids: evaluation of the effects at different biological organization levels, Ecotoxicol. Environ. Saf. 73 (2010) 1456–1464.
[58] G. Bhattacharya, R. Giri, A. Dubey, S. Mitra, R. Priyadarshini, A. Gupta, M. Mukhopadhyay, S. Ghosh, Structural changes in cellular membranes induced by ionic liquids: from model to bacterial membranes, Chem. Phys. Lipids 215 (2018) 1–10.
[59] G. Bhattacharya, R. Giri, H. Saxena, V. Agrawal, A. Gupta, M. Mukhopadhyay, S. Ghosh, X-ray reflectivity study of the interaction of an imidazolium-based ionic liquid with a soft supported lipid membrane, Langmuir 33 (2017) 1295–1304.
[60] G. Bhattacharya, S. Mitra, P. Mandal, S. Dutta, R. Giri, S. Ghosh, Thermodynamics of interaction of ionic liquids with lipid monolayer, Biophys. Rev. 10 (2018) 709–719.
[61] A. Aroti, E. Leontidis, E. Maltseva, G. Brezesinski, Effects of Hofmeister anions on DPPC Langmuir monolayers at the air − water interface, J. Phys. Chem. B 108 (2004) 15238–15245.
[62] M. Jurak, Thermodynamic aspects of cholesterol effect on properties of phospholipid monolayers: Langmuir and Langmuir–Blodgett monolayer study, J. Phys. Chem. B 117 (2013) 3496–3502.
[63] H. Brockman, Lipid monolayers: why use half a membrane to characterize protein-membrane interactions? Curr. Opin. Struct. Biol. 9 (1999) 438–443.
[64] M. Sadati, A.I. Apik, J.C. Armas-Perez, J. Martinez-Gonzalez, J.P. Hernandez-Ortiz, N.L. Abbott, J.J. de Pablo, Liquid crystal enabled early stage detection of beta amyloid formation on lipid monolayers, Adv. Funct. Mater. 25 (2015) 6050–6060.
[65] K. Birdi, Lipid and Biopolymer Monolayers at Liquid Interfaces, Springer Science & Business Media, 2013.
[66] K. Sabatini, J.-P. Mattila, P.K. Kinnunen, Interfacial behavior of cholesterol, ergosterol, and lanosterol in mixtures with DPPC and DMPC, Biophys. J. 95 (2008) 2340–2355.
[67] R.T. Azuah, L.R. Kneller, Y. Qiu, P.L. Tregenna-Piggott, C.M. Brown, J.R. Copley, R.M. Dimeo, DAVE: a comprehensive software suite for the reduction, visualization, and analysis of low energy neutron spectroscopic data, J. Res. Nat. Ins. Stand. Technol. 114 (2009) 341.
[68] D. Brown, E. London, Functions of lipid rafts in biological membranes, Annu. Rev. Cell Dev. Biol. 14 (1998) 111–136.
[69] K. Simons, E. Ikonen, Functional rafts in cell membranes, nature 387 (1997) 569.
[70] A.I. de Kroon, Metabolism of phosphatidylcholine and its implications for lipid acyl chain composition in Saccharomyces cerevisiae, Biochim. Biophys. Acta-Mol. Cell Biol. Lipid 1771 (2007) 343–352.
[71] R. Schneiter, V. Tatzer, G. Gogg, E. Leitner, S.D. Kohlwein, Elo1p-dependent Carboxy-terminal elongation of C14: 1Δ9 to C16: 1Δ11 fatty acids inSaccharomyces cerevisiae, J. Bacteriol. 182 (2000) 3655–3660.
[72] S.J. Labrie, J.E. Samson, S. Moineau, Bacteriophage resistance mechanisms, Nat. Rev. Microbiol. 8 (2010) 317.
[73] C. Schwechheimer, M.J. Kuehn, Outer-membrane vesicles from Gram-negative bacteria: biogenesis and functions, Nat. Rev. Microbiol. 13 (2015) 605.
[74] F.M. Klis, Cell wall assembly in yeast, Yeast 10 (1994) 851–869.